A Non-invansive and Self-managed Microscope for Predicting Radiation-Induced Acute Toxicities in Cancer Patients

Alessandra Catalano[1], Sophie Veronique Materne[1], Fabio Badenchini[2], Eliana La Rocca[3], Eliana Gioscio[1], Francesco Pisani[1], Luca Possenti[1], Barbara Avuzzi[5], Barbara Noris Chiorda[5], Carlotta Giandini[5], Riccardo Roy Colciago[5], Maria Carmen De Sanctis[5], Tommaso Giandini[4], Alessandro Cicchetti[1], and Tiziana Rancati[1]

[1]Data Science Unit, Fondazione IRCCS Istituto Nazionale dei Tumori, Milan, Italy
[2]Unit of GenitoUrinary Oncology, Fondazione IRCCS Istituto Nazionale dei Tumori, Milan, Italy
[3]Department of Radiation Oncology, University of Verona Hospital Trust, Verona, Italy
[4]Division of Medical Physics, Fondazione IRCCS Istituto Nazionale dei Tumori, Milan, Italy
[5]Department of Radiation Oncology, Fondazione IRCCS Istituto Nazionale dei Tumori, Milan, Italy

Abstract Microcirculation is the terminal vascular network of the systemic circulation. It has a pivotal role in the cardiovascular system. Damage to microvessels caused by radiotherapy (RT) contributes to toxicity development in a non-clarified manner. This work aims to investigate quantitatively the role of microcirculation in predicting acute toxicities after breast and prostate cancer RT. We enrolled 247 patients at a single centre for this study RT. We assessed the single-patient baseline microvasculature health status (MVHS) before RT using a microscope coupled to the GlycoCheck™ software. The system records videos (in the sublingual region) showing the live movement of red blood cells in the microvessels, analyses the microvasculature and computes the MVHS value for the overall health of microcirculation. We fitted a logistic model for the association between MVHS and acute toxicities, and we found a quantitative relationship between microvasculature health status and radio-sensitivity for patients both breast and prostate cancer patients.
The information obtained from the sublingual microscope could help personalise predictive models for toxicity and tailor them to the functional status of each patient.

1 Introduction

Microcirculation is an intricate network of arterioles, capillaries and venules that supply and drain blood from every tissue and organ in the body. The particular architecture of these microvessels varies depending on the specific structure of the vital organ they serve. An essential aspect of microcirculation is its pivotal role as the functional core of the cardiovascular system, facilitating the exchange of oxygen, carbon dioxide, nutrients, hormones, water and drugs, and as a causal factor in developing some pathologies.
Radiotherapy (RT) can contribute to microcirculation dysfunction. Indeed, the damage to the microcirculation causes endothelial cell dysfunction, increased vessel permeability and alterations in vasoconstriction and vasodilation, impacting oxygen and nutrient diffusion within the tumour and, consequently, the treatment efficacy. Moreover, RT also damages the microvessels of healthy organs, interfering with the damage recovery and toxicity manifestation process. Several trials have indicated an increased risk of normal tissue complications in patients with pre-existing medical conditions (hypertension, diabetes, use of cholesterol-lowering drugs, use of drugs for cardiac morbidity, obesity) or specific habits (smoking, alcohol abuse, low physical activity) that negatively impact the stability of the vascular system [1–5].
This work aimed to investigate quantitatively the role of microcirculation in predicting acute toxicities after breast (BCa) and prostate (PCa) cancer RT. Current RT techniques and plan optimisation for these two districts allow dose distributions highly conformed to the clinical targets, with small proportions of normal tissue receiving relevant doses. For these reasons, dose parameters are weakly associated with side effects, and the search for patient-specific features highlighting exceptional radiosensivity in still an active field of research. We included a quantitative measure of the single-patient microvascular health status (as measured by GlycoCheck™) in a predictive model for acute toxicities.

2 Materials and Methods

2.1 The study cohort

This prospective and observational study enrolled 247 patients between February 2021 and November 2023. The study cohort consisted of 143 BCa and 104 PCa patients. Women were treated with chemo RT in 25% of cases. RT was applied with a dose boost in 50% of treatments (33% as a sequential boost and 17% as a concomitant boost). Dose per fraction to PTV was 2.6-2.67 Gy in 85% of patients, 5.5 Gy in 10% of treatments and conventional 2 Gy for the remaining 5% of cases. Regarding prostate patients, 25% of them underwent adjuvant RT with 70 Gy in 35 fr. The remaining part was treated with a dose/fr in the 2-2.65 Gy range and a prescribed dose between 65 and 78 Gy.
Before RT, we trained patients to perform the baseline sublingual-microvasculature measurement (details in section 2.2). Clinicians collected the patient's condition at the baseline and at the RT end following CTCAE v4.0. We focused on the worst toxicity symptoms in each cohort, namely grade ≥ 2 erythema for BCa and simultaneous gastrointestinal (GI) and genitourinary (GU) grade ≥ 1 toxicity for PCa.

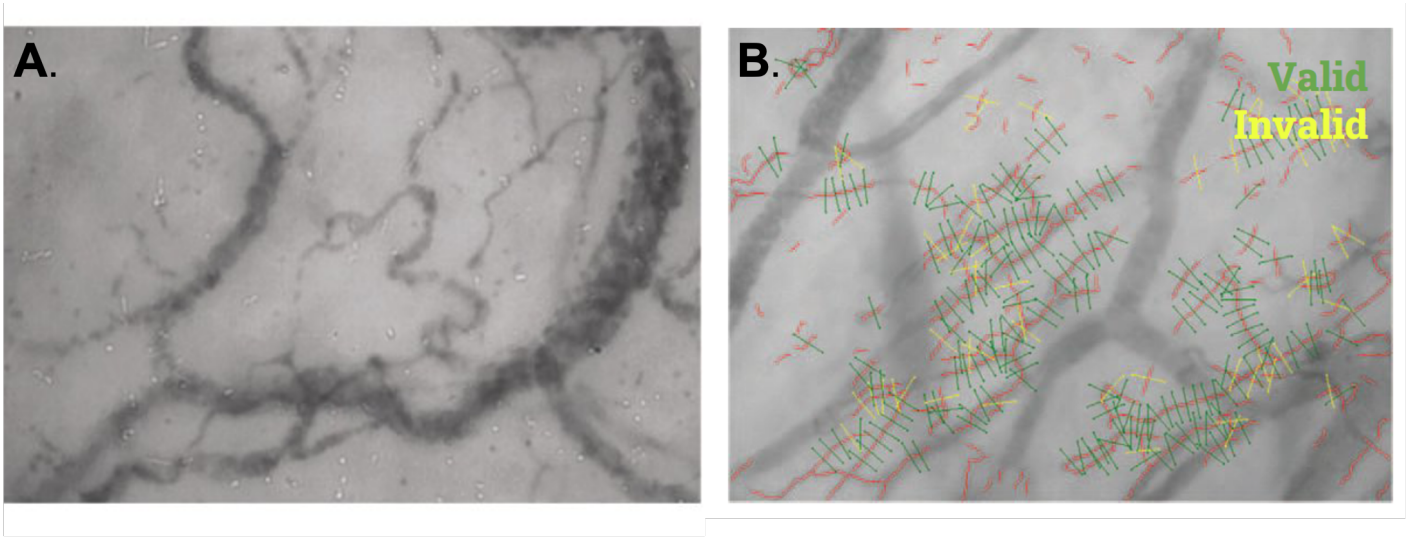

Figure 1: Glycocheck image acquisition. **A.** Frame of the videos recorded by the Glycocheck SDF Camera. **B.** After the image acquisition, the software automatically undergoes several quality check to select the vascular segments with sufficient quality for further analysis. Invalid segments (yellow) are distinguished from the valid vascular segments (green) [6].

2.2 The Instrument: Sublingual Video-Microscopy

The image acquisition of the sublingual microvasculature is performed through the GlycoCheck™ system. It comprises a handheld, non-invasive sidestream dark-field (SDF) camera coupled with a computer with the GlycoCheck software™ (GlycoCheck, Maastricht, the Netherlands). The SDF camera uses green light-emitting stroboscopic diodes (LED) to detect the haemoglobin of passing Red Blood Cells (RBC). The system acquires images in the sublingual region and extrapolates parameters representative of systemic microvascular health. The Glycocheck Software facilitates automatic image acquisition, identifying micro-vessels (with a thickness below 30 μm) during the process and analysing vascular segments along the length of the identified vessels. A single bench of measures consists of 40 frames encompassing 300 vascular segments. Next, the patient relocates the camera to a different position to record an additional acquisition. In this way, the spatial heterogeneity of the sublingual microcirculation is ensured. After acquiring images, the software analyses the vascular segments that satisfy predefined image quality criteria.
The software computes functional and morphological parameters, such as vessel diameter distribution, RBC velocity (VRBC), capillary density, capillary blood volume (CBV) and perfused boundary region (PBR) (see the Additional Material for equations).

2.3 Microvasculature Health Score

The crucial systemic measure obtained by the Glycocheck Software is the Microvascular Health Score (MVHS), which gives information about the overall health of the microvascular system. It is a synthetic and global score ranging from 0 to 15.
The MVHS computation uses all the functional and morphological parameters obtained during the recordings, such as the CBV, the capillary blood volume recruitment (CR) and the PBR [7]. More in detail, the software computes the ratio between the dynamic capillary blood volume CBV_{dyn} and PBR_{4-25} flow corrected (PBR_{4-25}-FL), so

$$MVHS_{dyn} = \frac{CBV_{dyn}}{PBR_{4-25} - FL}. \quad (1)$$

This parameter provides an overall quantitative evaluation of microvascular health. The higher the MVHS, the better the microvascular condition.

2.4 MVHS Imputation and Statistical analysis

The analysis focused on the association of MVHS with acute toxicity. MVHS summarises all the microcirculation parameters, and is automatically normalised for all patients.
The software's computation of MVHS needs a prolonged video acquisition, and it is not calculated for less compliant subjects. Consequently, we developed an imputation model to extrapolate the MVHS for patients with missing information. We based the imputation on all the available parameters. We trained the model on the entire population and tested the results on patients with the GlycoCheck™ computed MVHS. The training process was iterated until the average error between the observed and the imputed values was below 0.05.

3 Results

Forty-one/143 (28.7%) BCa patients developed grade ≥ 2 skin erythema. Sixty-three/104 (60.6%) PCa patients experienced grade ≥ 1 in both GI and GU domains.
The GlycoCheck exam was self-performed by patients. MVHS, requiring a longer video registration, was calculated

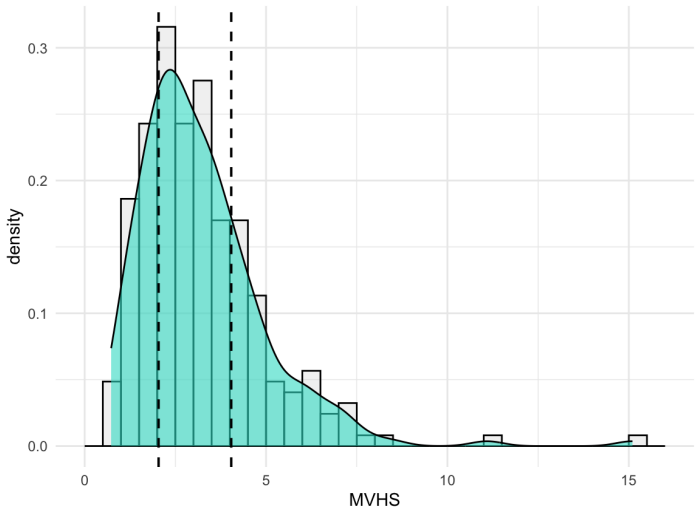

Figure 2: Density plot for the MVHS. The dashed lines represent the 1st and the 3rd quartile of MVHS distribution.

for 60% of patients, while it was obtained by multiple imputation models for the remaining part. After 250 iterations, the model reached good stability with an average error between the predicted and the observed value of MVHS equals -0.04, making the imputed values reliable.

The median MVHS was 2.87, and the 1st and 3rd quartiles were 2.04 and 4.04, respectively (see Figure 2 for the whole distribution). Stratifying for cancer type, the median MVHS was 3.06 in the BCa and 2.75 in PCa.

The logistic model coefficients were $\beta_0 = 0.58$ (constant), $\beta_1 = -0.29$ (slope for MVHS, $OR = 0.81$ for one point increase in MVHS; $p - value = 0.002$). As expected, a higher MVHS (i.e., a healthy microcirculation) protects from side effects. MVHS box plots for BCa and PCa patients stratified for acute toxicity are depicted in Figure 3.

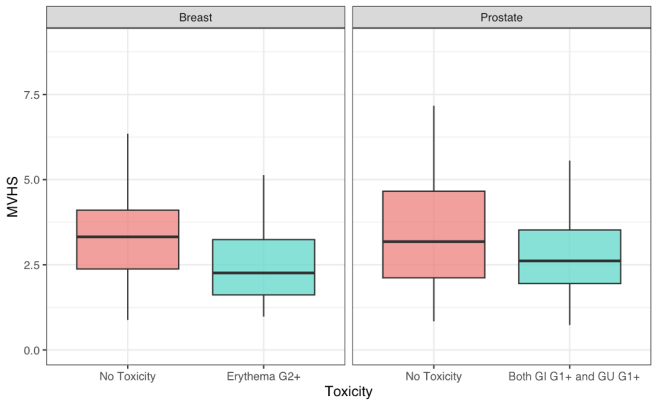

Figure 3: Distribution of MVHS between the two cohorts of patients and separated for toxicity (both $p - value < 0.0001$)

4 Discussion

We tested and quantitatively assessed the MVHS through a non-invasive tool and established the relationship between the microvasculature condition and acute radiation-induced toxicity in a cohort of BCa and Pca patients. The model confirmed an association between altered microvasculature and the damage repair mechanisms following RT, independently from the treatment region and patient sex. Indeed, MVHS distributions for breast and prostate populations were similar (p-value from t-test = 0.36), showing a negligible impact due to sex. In contrast, MVHS distributions for patients experiencing toxicity were significantly different in both the cancer cohorts (p-value <0.0001 in both cases).

From a quantitative point of view, a reduction of 1 value in the MVHS scale corresponded to an (averaged) increased risk of 23.5% of developing radiation-induced symptoms. We can define three risk classes by stratifying patients through the clinical definition of MVHS (see points of Figure 4). The low-risk group (patients having MVHS higher than 4) in which the probability of developing toxicity is 28%; the second class, representing the average patient (MVHS between 2 and 4), is at moderate risk with a toxicity rate equal to 41%. The last class (MVHS less than 2) with compromised microcirculation had a toxicity rate of 59%.

A new analysis is ongoing, including a cohort of 75 head-neck cancer patients and investigating dysphagia, xerostomia and mucositis. Considering the heterogeneity of RT treatments (and dose distributions in organ at risk) in these patients, we will include the MVHS in dose-response models for this cohort.

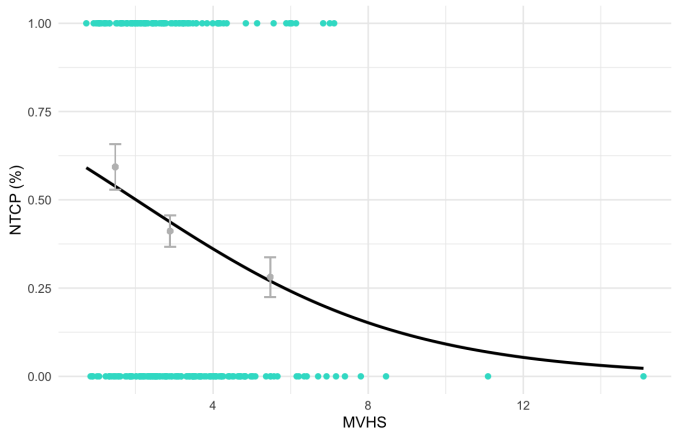

Figure 4: Normal Tissue Complication Probability as a function of MVHS. The three points show the three risk classes (low, moderate and high risk).

5 Conclusion

The study highlights the possibility of implementing a non-invasive instrument in clinical practice to gather information about microcirculation status and define the toxicity risk in different tumour districts using a patient-specific MVHS. The MVHS model predicts acute toxicity, proving a quantitative relationship between microvasculature status and radio-sensitivity in an organ-agnostic way.

The systemic functional information derived by the sublingual microscope could boost the personalisation of predictive models and tailor them to the single-patient functional status.

6 Acknowledgments

The study was supported by AIRC Investigator Grant no. 21479.

6.1 Additional material: formulas

The GlycoCheck software computes two categories of parameters: those specific to each vessel diameter class and those calculated across all diameter classes ranging from 4 to 25 μm, yielding a singular value for each subject's measurement.
Within the first category are three parameters. First, the capillary density, the RBC velocity (VRBC), and the perfused boundary region (PBR). In the second category, the GlycoCheck Software computes the microvascular blood flow, the total valid perfused microvascular density, and the parameters essential for deriving the microvascular health scores. They are the relative capillary blood volume absolute, relative, static and dynamic. In formulas:

$$CBV_{abs} = \ capillary\ density * \pi r^2$$

$$CBV_{rel} = \frac{VRBC(D \geq 10\mu m)}{VRBC(D \leq 7\mu m)}$$

$$CBV_{stat} = CBV_{abs} * CBV_{rel}$$

$$CR = 1 - slope(VRBC(D \leq 7\mu m), VRBC(D \geq 10\mu m))$$

$$CBV_{dyn} = CBV_{stat} * (1 + CR).$$

The static PBR (PBR_{4-25}) is the average PBR calculated across all diameter classes, while the dynamic PBR (PBR_{4-25} flow corrected) is the PBR_{4-25} with $VRBC(D \geq 10\mu m)$ set to 0. This minimises the possible flow-dependent variability in the PBR estimation, as the RBC penetration into the luminal glycocalyx surface can be velocity-dependent.

References

[1] M. D. Santis, F. Bonfantini, F. D. Salvo, et al. "Factors influencing acute and late toxicity in the era of adjuvant hypofractionated breast radiotherapy." *The Breast* 29 (2016), pp. 90–95. DOI: 10.1016/j.breast.2016.07.013.

[2] F. Palorini, T. Rancati, C. Cozzarini, et al. "Multi-variable models of large International Prostate Symptom Score worsening at the end of therapy in prostate cancer radiotherapy." *Radiother Oncol.* 118 (Jan. 2016), pp. 92–8. DOI: 10.1016/j.radonc.2015.11.036.

[3] D. G, V. den Bergh L, A.-M. A, et al. "The benefits of including clinical factors in rectal normal tissue complication probability modeling after radiotherapy for prostate cancer." *Int J Radiat Oncol Biol Phys.* 82 (Mar. 2012), pp. 1233–42. DOI: 10.1016/j.ijrobp.2011.03.056.

[4] S. Tucker, L. Dong, W. Bosch, et al. "Late rectal toxicity on RTOG 94-06: analysis using a mixture Lyman model." *Int J Radiat Oncol Biol Phys.* 78 (Nov. 2010), pp. 1253–60. DOI: 10.1016/j.ijrobp.2010.01.069.

[5] C. Anna, R. Tiziana, C. Alessandro, et al. "EP-1594: Development of multivariable models for acute toxicities in nasopharyngeal cancer radiotherapy". *Radiotherapy and Oncology* 123 (May 2017), S858–S859. DOI: 10.1016/S0167-8140(17)32029-7.

[6] D. Lee, B. D. M. van den Berg, M. Boels, et al. "Deeper Penetration of Erythrocytes into the Endothelial Glycocalyx Is Associated with Impaired Microvascular Perfusion." *Phys Med Biol* (2014). DOI: https://doi.org/10.1371/journal.pone.0096477.

[7] Rovas, A., Sackarnd, et al. "Identification of novel sublingual parameters to analyze and diagnose microvascular dysfunction in sepsis: the NOSTRADAMUS study." *Crit Care 25* 112 (2021). DOI: https://doi.org/10.1186/s13054-021-03520-w.